# Dorsorostral Snout Muscles in the Rat Subserve Coordinated Movement for Whisking and Sniffing

**SEBASTIAN HAIDARLIU,[1]* DAVID GOLOMB,[2,3] DAVID KLEINFELD,[4] AND EHUD AHISSAR[1]**

[1]Department of Neurobiology, The Weizmann Institute of Science, Rehovot, Israel
[2]Department of Physiology and Zlotowski Center for Neuroscience, Ben-Gurion University of the Negev, Beer-Sheva, Israel
[3]Janelia Farm Research Campus, Howard Hughes Medical Institute, Ashburn, Virginia
[4]Department of Physics and Section of Neurobiology, University of California, San Diego, La Jolla, California

ABSTRACT

Histochemical examination of the dorsorostral quadrant of the rat snout revealed superficial and deep muscles that are involved in whisking, sniffing, and airflow control. The part of *M. nasolabialis profundus* that acts as an intrinsic (follicular) muscle to facilitate protraction and translation of the vibrissae is described. An intraturbinate and selected rostral-most nasal muscles that can influence major routs of inspiratory airflow and rhinarial touch through their control of nostril configuration, atrioturbinate and rhinarium position, were revealed. Anat Rec, 295:1181–1191, 2012. © 2012 Wiley Periodicals, Inc.

**Key words: active sensing; breathing; nose muscles; rodents**

Rodents with poor vision and nocturnal activity rely heavily on senses of touch and smell. In the rat, whisking and sniffing are iterative cyclic motor features that accompany active tactile and olfactory sensing, respectively. The whisking and sniffing rhythms can couple during exploratory behavior (Welker, 1964; Komisaruk, 1970; Kepecs et al., 2007; Wachowiak, 2011; Deschênes et al., 2012). Moreover, tactile sensation can also be acquired via the rhinarium (Brácha et al., 1990), which is covered with glabrous skin and has a dense sensory innervation (Macintosh, 1975; Silverman et al., 1986). Muscle contraction is the principal action that determines whisking, sniffing, and changes of the nostril configuration. Most whisking parameters (Carvell and Simons, 1990; Berg and Kleinfeld, 2003; Towal and Hartmann, 2006; Knutsen et al., 2008), as well as other types of movements such as translation of the vibrissae and of the entire mystacial pad (MP) (Bermejo et al., 2005; Hill et al., 2008; O'Connor et al., 2010), are determined relative to the rat's head. Recently, we summarized data regarding the architecture of the muscles associated with the rat MP (Haidarliu et al., 2010). However, the muscles in the dorsorostral quadrant (DRQ) of the rat snout were poorly illuminated. Although many of the snout muscles of rodents were frequently described, and their aggregate electromyogenic activity recorded (Carvell et al., 1991; Berg and Kleinfeld, 2003; Hill et al., 2008), the specific actions of many of these muscles remain unclear.

According to the map of muscles in the MP described by Dörfl (1982), and to known mechanical models of the rat MP (Wineski, 1985; Hill et al., 2008; Simony et al., 2010; Haidarliu et al., 2011), each large vibrissa is protracted by two intrinsic muscles (IMs). However, the rostral-most vibrissae A4 and B4 are attached to only

Abbreviations used: AT=atrioturbinate; DRQ=dorsorostral quadrant; IM=intrinsic muscle; ITM=intraturbinate muscle; MP=mystacial pad; PIM=pseudointrinsic muscle.

Grant sponsor: European Commission; Grant number: BIOTACT (ICT-215910); Grant sponsors: The Minerva Foundation funded by the Federal German Ministry for Education and Research; The National Institutes of Health; Grant number: NS058668; Grant sponsor: United States–Israel Binational Science Foundation; Grant number: 2007121.

*Correspondence to: Sebastian Haidarliu, Department of Neurobiology, The Weizmann Institute of Science, Rehovot 76100, Israel. Fax: 972-8-9346099. E-mail: sebastian.haidarliu@weizmann.ac.il

Received 13 November 2011; Accepted 3 May 2012.

DOI 10.1002/ar.22501
Published online 29 May 2012 in Wiley Online Library (wileyonlinelibrary.com).

one IM, which might be not sufficient for the protraction amplitude of these vibrissae to be the same as that for vibrissae protracted by two IMs. Nonetheless, during whisking, all the vibrissae of the MP, including the A4 and B4 vibrissae, whisk synchronously and with similar amplitudes (Carvell and Simons, 1990; Bermejo et al., 2005; Hill et al., 2011). Such movement synchrony along whisker arcs is important for encoding the spatial coordinates of object location (Ahissar and Knutsen, 2008; Knutsen et al., 2008; Knutsen and Ahissar, 2009). Detection of a structure in the DRQ that could act as the missing IM for the A4 and B4 vibrissae was an impetus for our study of the muscular organization of the DRQ.

Rats are obligate nose breathers, with inspired and expired air passing only through their noses (Krinke, 2000). The shape of their nose is maintained by the bony and cartilaginous nasal skeleton. The rat nose has a dynamic structure and a specific external and internal organization (Bojsen-Moller and Fahrenkrug, 1971; Maier, 2002). The rat rhinarium has a dense sensory innervation (Silverman et al., 1986), and participates in tactile exploration. This participation was observed in experiments that required a rat to reach with its head, in which a decision was made after a rat touched a feeder entrance with the tip of its nose (Brácha et al., 1990). Traffic of the air during sniffing is under the control of relevant muscles that can change the nostril configuration and the position of the rhinarium. Usually, these muscles contract synchronously with the MP muscles, and can change the shape of the air conducting structures, such that the re-inhalation of the expired air is reduced (Haselton and Sperandio, 1988; Wilson and Sullivan, 1999; Kepecs et al., 2006). Thus, another aim of this study was identification of the muscles that can cause movements of the nostril and rhinarium, which would influence nasal aerodynamics and rhinarium-mediated active tactile sensing in rats.

Classical descriptions of the rodent snout musculature mainly involved tissue dissection. In the rodent snout, many parts of the *M. nasolabialis profundus* have been described and compared. However, the names, as well as data on their relative development, size, origin, and exact insertion sites, for these parts are not the same in all the studies. Such diversity was attributed to the difficulties of rodent snout dissection (Rinker, 1954). Despite the diversity of opinions in the literature concerning the names and specific anatomical arrangement of facial muscles in humans and other mammals, similarities in their overall form, origin, and insertions suggest homologies between species (Banke et al., 2001; Breitsprecher et al., 2002; Whidden, 2002). In an anatomical study of the nasal superficial musculoaponeurotic system, the surgical approach was thought to cause disruption of the anatomical nasal structures (Saban et al., 2008). Indeed, microdissection of individual muscle fibers showed that such a procedure can cause a sudden contraction of the dissected muscle fibers, making further muscle separation impossible (Huijing, 1999). To surmount these past difficulties, we felt that histochemical visualization and mapping of small muscles in the rat DRQ *in situ* might be more advantageous for mapping numerous small muscles than traditional dissection method or the recent "face mask" technique (Diogo et al., 2009).

Our goal was to update and expand our knowledge of the muscle distribution and function in the DRQ by applying special histological techniques. Serial sectioning in different planes and muscle visualization *in situ* permitted us to make the initial description of the rhinarial, intraturbinate, and pseudointrinsic muscles (PIMs), and to identify three distinctive and spatially separated areas of muscle origins in the rostral part of the rat snout. For the *M. dilator nasi*, an additional function was revealed that consists in nose retraction and vibrissa protraction which are characteristic for the first stage of the sniff cycle. The muscles we describe may participate in the control of sniffing, whisking, and active tactile and olfactory sensing.

## MATERIALS AND METHODS

Rostral snout musculature of 16-male albino Wistar rats between 4 months and 1-year old was examined. In addition, six 1-week-old rats were used for preparation of the whole head slices to reveal the attachment of muscles to the skull; these could not be obtained from adult rats without decalcification. All the experimental procedures were conducted according to NIH standards and were approved by the Institute Animal Care and Use Committee at the Weizmann Institute of Science. Rats were anesthetized intraperitoneally with urethane [25% (w/v); 0.65 mL/100 g body weight], perfused transcardially with 4% (w/v) paraformaldehyde and 5% (w/v) sucrose in 0.1 M phosphate buffer, pH 7.4, and then decapitated. Entire heads and lateral snout flaps were postfixed in the solution used for perfusion, to which additional [25% (w/v)] sucrose was added. Muscles of the snout were visualized after staining for cytochrome oxidase activity as strongly stained in dark-brown structures that contained oxidized deposited diaminobenzidine, as previously described (Haidarliu et al., 2010). Briefly, muscle arrangement was revealed *in situ* in histological slices sectioned with a freezing microtome (SM 2000R; Leica Instruments, Germany) in different planes, that is, coronal, parasagittal or tangential, horizontal, and oblique. The first three planes are used to determine stereotaxic coordinates of different brain structures. The oblique plane, vertical and $\sim 45^{\circ}$ to both coronal and sagittal planes, was used mainly to reveal rhinarial musculature. For coronal and horizontal slicing, rostral parts of the snout were excised and subjected to postfixation for 48 hr. Tangential slicing was used to reveal the muscles with their attachment sites in the rhinarium, within the entire DRQ, and in adjacent parts of the MP. Tissue flaps that contained rostral part of the snout starting from the philtrum and hemirhinarium, together with the MPs, were flattened in RCH44 perforated plastic histology cassettes (Presctech.com) to prevent curling during dehydration caused by the postfixation. The flaps were frozen and sliced as a single straightened histological preparation, and the slices were stained for cytochrome oxidase and cover-slipped with Kristalon (Harleco; Lawrence, KS). Structures containing collagen were visualized by fluorescence microscopy for blue autofluorescence as described (Haidarliu et al., 2011).

Borders of the DRQ relative to the bony landmarks and vibrissae were determined with X-ray digital radiovisiography (Gendex Dental Systems, Des Planes, IL) of the rat head in a sagittal plane. Images of the nasal

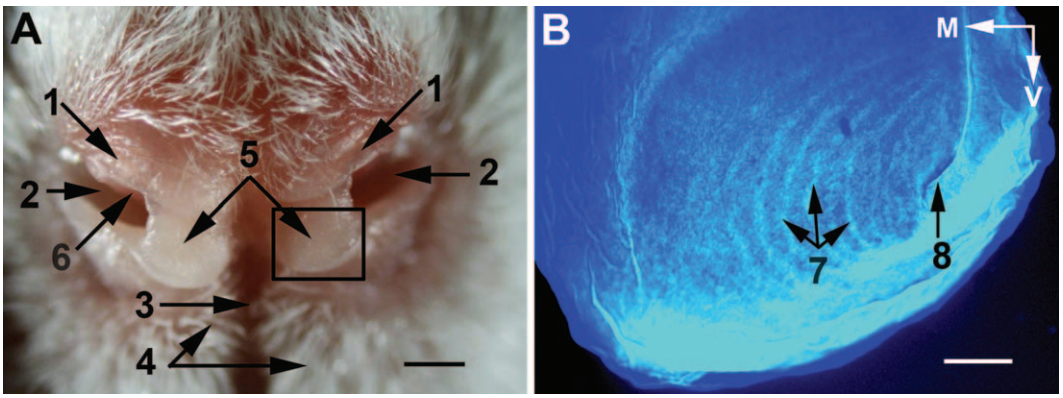


Fig. 1. Morphology of the rat rhinarium. (**A**) Anterior view of the rat rhinarium. Boxed area shows the borders of the region that corresponds to (**B**) after this rat snout was subjected to histological treatment. (B) Autofluorescence of a nasal tubercle superficial slice (60-μm thick) stained for cytochrome oxidase activity. 1, Regio suprarhinarica; 2, nostrils; 3, sulcus medianus (philtrum); 4, paramedian ridges; 5, nasal tubercles (pads); 6, atrioturbinate; 7, epidermal (friction) ridges arranged as a whorl, with the centre of the whorl (8) in the ventrolateral part of each tubercle. M, medial; V, ventral. Scale bars are 1 mm in (A) and 0.2 mm in (B).

turbinates were obtained by direct photography of the lateral walls of the nasal cavity in young, that is, 1-week old, and adult rats.

For one of the largest muscles of the rat snout whose insertion site is within the DRQ (*M. dilator nasi)*, the effect of direct electrical stimulation of the muscle belly was studied. Intramuscular electrical stimulation was applied through the tungsten microelectrodes (125-μm shaft diameter, ~30-μm tip diameter), that were inserted through the skin and directed toward muscle belly. The position of the electrode was adjusted using a stereotaxic device (SR-6; Narishige, Tokyo, Japan). The stimulus (AC, 10 V, 50 Hz) was applied for 1–2 s to obtain a sustained contraction. Similar voltages were used to stimulate individual facial muscles in humans and monkeys (Waller et al., 2006), as well as to elicit visible contractions of the vibrissa muscles in rats (Sinis et al., 2009). To verify the position of the electrode tip, a stronger current (AC, 20 V, 50 Hz, 4 s) was applied, and the same histochemical method was used to visualize the lesion site.

A Nikon Eclipse 50i fluorescent microscope, equipped with low magnification objectives of 2× and 1×, was used to obtain bright-field and autofluorescence images that were subsequently imported into Adobe Photoshop software (version CS) for the preparation of figures. Only minimal adjustments in the contrast and brightness of the images were made.

## RESULTS

### Muscles Involved in Control of Nostril and Nose Movements

The rostral-most prominent part of the rat nose, known as the rhinarium, contains the nostrils (Fig. 1). In highly magnified photographs of the rhinarium, nostrils were directed caudolaterally, and were separated by nasal tubercles. Nasal tubercles were prominent and covered with epidermal ridges of which circular arrangement was seen both by light and fluorescent microscopy, and was reminiscent of the whorls characteristic for fingerprints (Fig. 1B). This finding is consistent with the pattern of ridges revealed on the snout pad surfaces after treatment with India ink by Macintosh (1975). In the

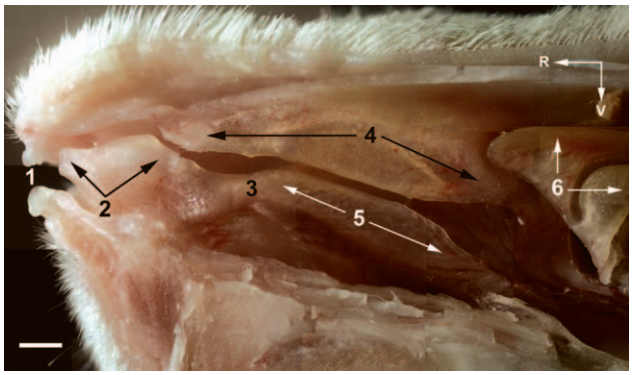


Fig. 2. Light microscopy of the right lateral wall in the nasal cavity of an adult rat. 1, Nostril; 2, atrioturbinate; 3, isthmus; 4, nasoturbinate; 5, maxilloturbinate; 6, ethmoturbinates. R, rostral; V, ventral. Scale bar = 1 mm.

rostral region of the rhinaria, nostrils had a semicircular shape. Caudally, they narrowed, and had a slit-like shape. Within the vestibulum nasi, the rostral edge of the atrioturbinate (AT), described by Silverman et al. (1986) as a prominent bulge, crossed the vestibulum at an angle of ~45° to the sagittal plane. Within the nasal cavity, AT extended caudally for ~2 mm, then continued in the caudal direction for another 5–6 mm now designated as maxilloturbinate (Fig. 2).

In the DRQ of adult rats, only soft tissues were represented (Fig. 3A). To preserve the cytochrome oxidase activity, histological slicing of the entire DRQ was performed with a freezing stage on the microtome and without preliminary decalcification. The borders of the DRQ were distinct in tangential slices of the rat snout (Fig. 3B). The DRQ was located rostral to the MP, and appeared limited caudally by a vertical plane passing through the forth vibrissal arc, and ventrally, by a horizontal plane passing through the vibrissal rows C. The DRQ possesses a complex structural organization of the muscles that is schematically shown in the Fig. 4.

Structures that might initiate movements of the rhinarium and nose, that is, lateral and vertical deflections,

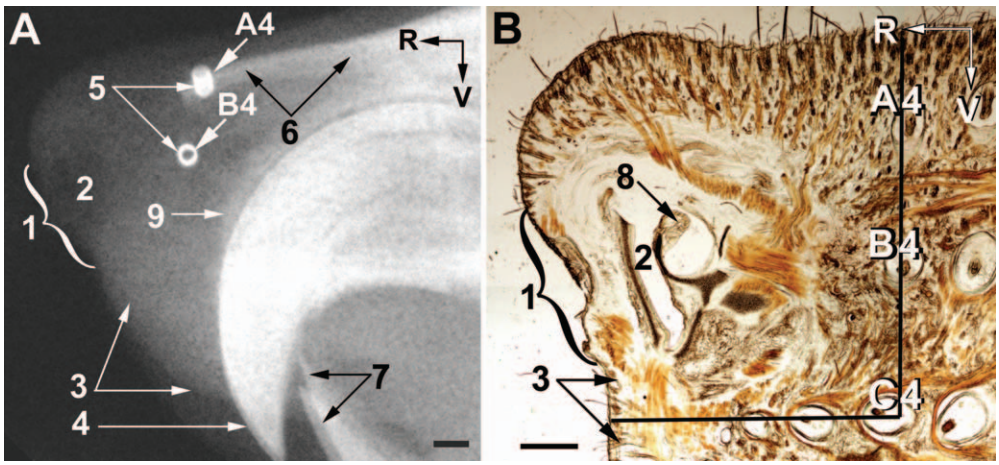


Fig. 3. A sagittal radiovisiogram of the rostral area of the head (**A**), and light microscopy of a parasagittal snout slice stained for cytochrome oxidase activity (**B**) in adult rats. Black lines in (B) show the borders of the DRQ. 1, Rhinarium; 2, nostril; 3, upper lip; 4, upper incisives; 5, short pieces of stainless steel tubes threaded by the A4 and B4 vibrissae at their proximal ends; 6, nasal bones; 7, lower incisives; 8, atriturbinate; 9, rostral pole of the premaxilla. R, rostral; V, ventral. Scale bars = 1 mm.

as well as retraction, were studied in horizontal and tangential slices of the rat snout. In the dorsal-most horizontal slices of the DRQ, the origin of the *M. transversus nasi* was seen along the midline on the dorsum nasi (Fig. 5) which is consistent with the classical descriptions of this muscle in rodents (Rinker, 1954). Muscle fibers were directed laterally, then ventrally, and inserted into the corium of the rostral part of the upper lip, and into dorsal part of the MP bilaterally. Muscle insertions into the upper lip corresponded to the atrial part of the nose. Thus contraction of the *M. transversus nasi* might pull the upper lip dorsally, which will also result in a slight caudodorsal shift of the rhinarium.

In horizontal slices cut at vibrissa row A, a large muscle, known as *M. dilator nasi* (Meinetz, 1944; Klingener, 1964; Ryan, 1989), was revealed (Fig. 6). This muscle originated from the maxilla, rostral to the edge of the Foramen infraorbitale, and from the dorsal surface of the zygomatic plate, and was inserted by a thin flat tendon into the aponeurosis above the nasal roof cartilage (Fig. 7A). Based on the geometry of the entire *M. dilator nasi*, which is clearly seen in a horizontal slice of the rat head, and on the direction of its numerous muscle fibers and long tendon, a function of this muscle might be lateral deflection and/or retraction of the nose in addition to a previously defined nostril dilatation. Nose deflections caused by the *M. dilator nasi* might be much quicker and more precise than the nose movements caused by turning the entire head for enlarging the field of the air sampled during sniffing. This conjecture was supported by data obtained during unilateral and bilateral electrical stimulation of the *M. dilator nasi* in anesthetized rats (Fig. 7B). Unilateral stimulation resulted in a slight rhinarium retraction and turning of the nose to the side of stimulation, with simultaneous ipsilateral protraction of the rostral vibrissal arcs (Fig. 7C,D). Bilateral stimulation resulted in retraction and a slight dorsal deflection of the nose tip and bilateral vibrissa protraction that imitated the first stage of the sniff cycle.

Slicing of the snout in an oblique plane that lay parallel to the edges of the nasal openings and at an angle of ~45° to the sagittal plane, revealed two muscles that might move the nose (rhinarium) in the vertical plane (Fig. 8A). The rostral muscle strip originated from the rhinarium, and the caudolateral muscle strip from the septum nasi and ventromedial part of the lateral nasal cartilage. The fibers of both these muscles were directed ventral, and passed rostral to the origins of the Partes mediae superior et inferior of the *M. nasolabialis profundus* (Fig. 8B). In coronal slices of the DRQ (Fig. 8C), it was seen that these fibers were inserted into the rostral part of the upper lip close to the philtrum bilaterally. Contraction of these two, previously unnamed muscles will pull the rhinarium and the ventral wall of the nostrils ventrally, simultaneously uplifting the rostral part of the upper lip, and resulting in nostril dilatation. We propose naming the new muscles *M. depressor rhinarii* and *M. depressor septi nasi.*

In the rostral-most coronal slices, in the middle of the dorsal part of the rhinarium, a tiny muscle was observed (Fig. 9A) that originated from the glabrous skin of the dorsal half of the rhinarium. It extended from the border with the nasal tubercles, and was inserted into the skin of the dorsum nasi (Fig. 9B). This muscle can pull the rhinarium dorsally. We propose to name it *M. levator rhinarii.*

## Muscles of the DRQ Involved in Vibrissa Movements

Superficial slices of the DRQ contained epidermis, roots of pelage hairs, multiple interlacing muscle fibers, a mesh of fibrillary elements of connective tissue, and four to six nasal vibrissae (Fig. 10A). In a few following slices, pelage hairs disappeared, and muscle fibers of the *Mm. nasolabialis et maxillolabialis* were observed coming from the caudal between rows of vibrissae (Fig. 10B). In these slices, highly divergent fibers of the posterior slips of the Pars interna of the *M. nasolabialis profundus*, like ones previously described in cricetid rodents (Rinker, 1954), also appeared from the rostral and were inserted into the corium of the MP of the rats (Fig. 10B).

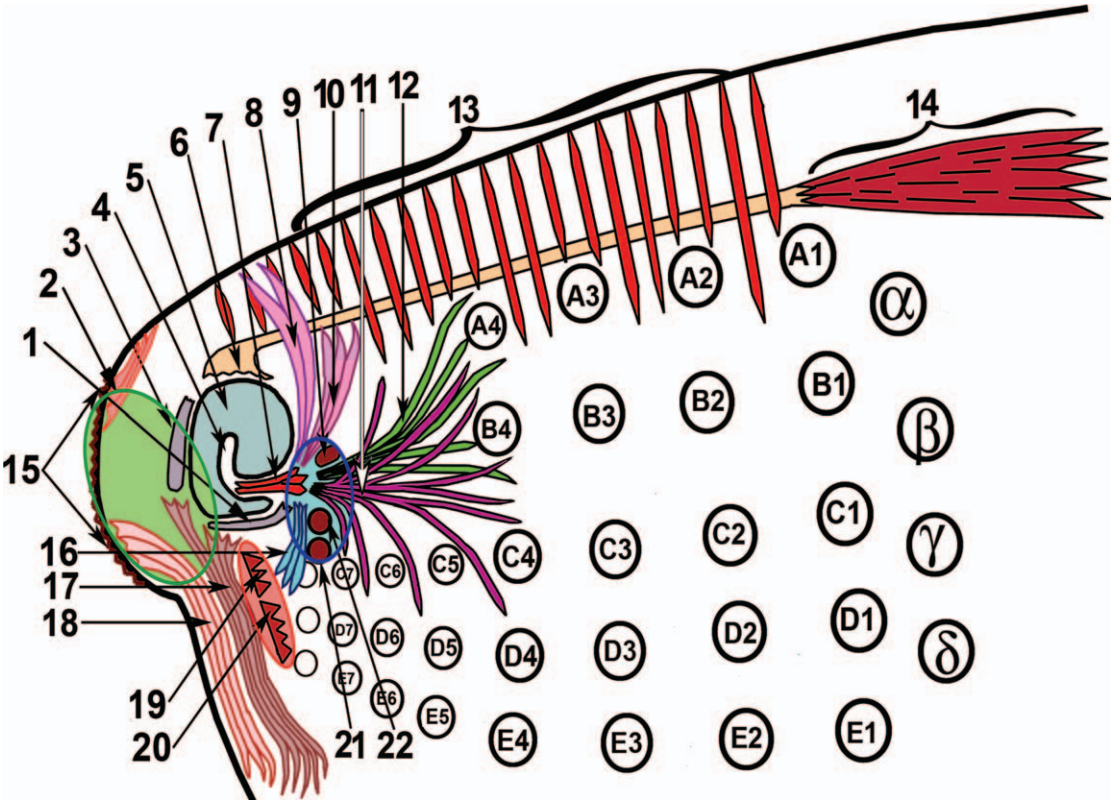


Fig. 4. Schematic representation of muscles related to the dorsorostral part of the rat snout. Encircled areas comprise origins of the following muscles: green area, rhinarial muscles; pink area, two extrinsic whisker protractors; and blue area, most of the parts of the *M. nasolabialis profundus.* 1, Ventromedial part of the lateral nasal cartilage; 2, *M. levator rhinarii*; 3, septal cartilage; 4, atrioturbinate; 5, atrium; 6, insertion site of the *M. dilator nasi*; 7, ITM; 8, 10, 11, and 12, the most superficial, superficial, posterior, and pseudointrinsic portions, respectively, of the Pars interna of the *M. nasolabialis profundus*; 9, origin of the Pars interna profunda; 13, *M. transversus nasi*; 14, belly of the *M. dilator nasi*; 15, rhinarium; 16, Pars anterior of the *M. nasolabialis profundus*; 17, *M. depressor septi nasi*; 18, *M. depressor rhinarii*; 19 and 20, origins of the Partes mediae superior et inferior, and 21 and 22, of the Partes maxillares profunda et superficialis, respectively, of the *M. nasolabialis profundus.* Marked black circles represent mystacial vibrissae.

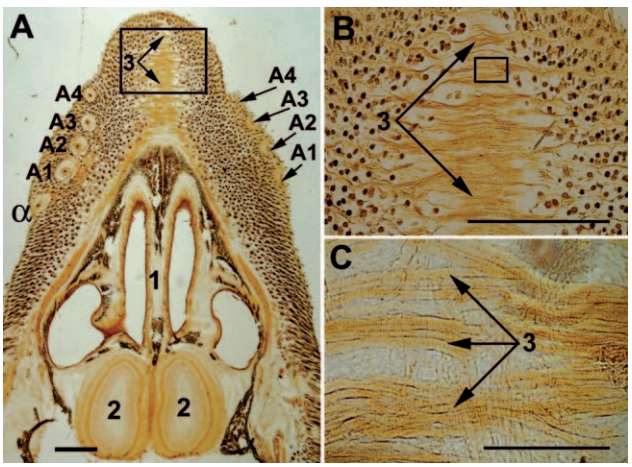


Fig. 5. Light microscopy of a horizontal slice of the dorsal part of a 1-week-old rat snout. (**A**) A slice of the whole snout; (**B** and **C**), higher magnifications of the boxed areas in (A) and (B), respectively. α, the dorsal-most straddler; A1–A4, the dorsal-most row of vibrissae. 1, Septum; 2, olfactory bulb; 3, striated fibers of the *M. transversus nasi.* Scale bars are 1 mm in (A) and (B), and 0.1 mm in (C).

In the DRQ, the fibers of these two muscle groups (the *Mm. nasolabialis et maxillolabialis* and Pars interna of the *M. nasolabialis profundus*) interdigitated, and in some places interconnected with each other.

In the next four to five slices, a separate muscle slip was seen that, according to Rinker (1954), might also belong to the most posterior part of the Pars interna of the *M. nasolabialis profundus* (Fig. 11). This muscle slip originated from the lateral wall of the nasal cartilage, passed 1–2 mm caudally, and fanned into a few bundles. Some of the bundles were directed toward the vibrissa follicles of rows A and B. Small fascicles of such bundles, each of which were composed of a few muscle fibers, were attached to the capsules of the A4 and B4 vibrissae (Fig. 12). Other muscle fibers passed toward the corium in close vicinity to rows A and B of vibrissae in the MP, and formed rosette-like contacts with the superficial collagenous layer of the skin. A part of the fibers of the Pars interna of the *M. nasolabialis profundus* was directed ventrocaudal, and was inserted into the skin in vicinity of the vibrissae in rows C and D (Fig. 10B). Capsular attachments of this part of the muscle in the rows C or D were not observed. Therefore, these muscle slips, in addition to the Partes mediae superior et inferior of the *M. nasolabialis profundus*, can participate in vibrissa

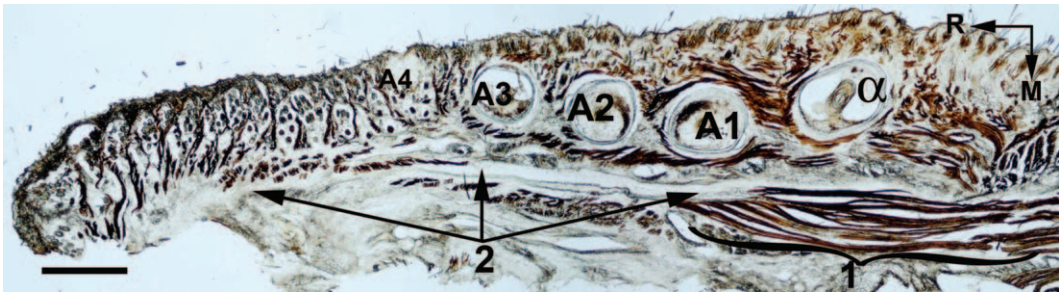


Fig. 6. Light microscopy of a horizontal slice of an adult rat snout in the plane of the vibrissa follicles in row A. α, follicle of the dorsal-most straddler; A1–A4, vibrissa follicles of row A; M, medial; R, rostral. 1, belly and 2, tendon of the *M. dilator nasi.* Scale bar = 1 mm.

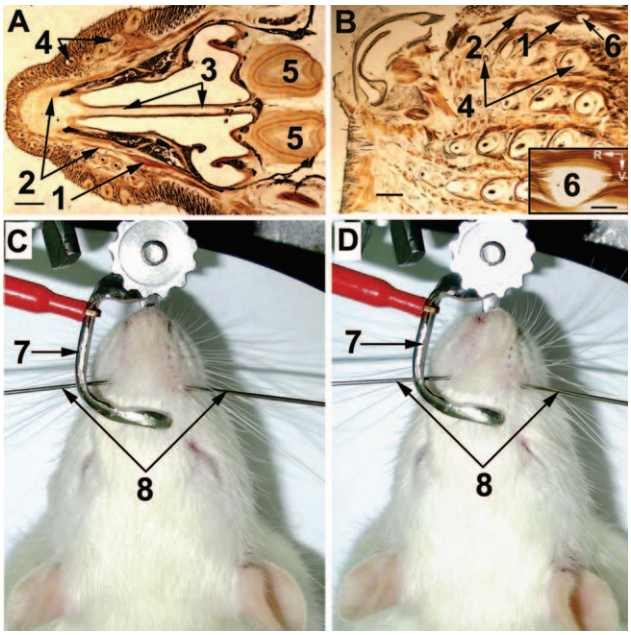


Fig. 7. Anatomical location and effect of electrical stimulation of the *M. dilator nasi.* (**A**) Horizontal slice of the head of a 7-day-old rat. 1, Belly and 2, tendon of the *M. dilator nasi;* 3, septum; 4, vibrissa row A; 5, olfactory bulb. Scale bar = 1 mm. (**B**) Light microscopic view of a snout tangential slice that contains an electrolytic lesion (6) caused by stimulating electrode in the belly of the *M dilator nasi* (1) in an adult rat. Inset: higher magnification of the lesion site (6). R, rostral; V, ventral. Scale bar = 0.2 mm. (**C**) Anesthetized rat with the head fixed in a stereotactic device. 7, Nasal piece of the head holder without ear bars; 8, guides that contain muscle stimulating electrodes. (**D**) Nose deflection during electrical stimulation (AC, 10 V, 50 Hz) of the right *M. dilator nasi.*

protraction and can diminish the vertical spread of the vibrissae during protraction of the vibrissae, as previously described (Sachdev et al., 2002; Brecht et al., 2006; Grant et al., 2009).

Until now, only IMs were known to attach directly to the vibrissa capsules. One of the slips of the P. interna of the *M. nasolabialis profundus* can be considered a PIM, based on its origin from the nasal cartilage and its insertion into the vibrissa capsules and surrounding corium (Figs. 11 and 12). Its belly was seen in only a few consecutive parasagittal slices, that is, up to five, 60-μm thick slices, of the rat snout. The PIM insertion sites were seen on both the distal, as well as on the central segments of the follicle, close to the slings of the relevant IMs. Thus, this muscle can participate in vibrissa protraction, as well as in its translation.

In deeper slices of the DRQ, the fibers of the third layer, that is, the fibrous mat, of the MP collagenous skeleton passed mainly in the rostrocaudal direction. More medial, muscle fibers of the Pars interna profunda of the *M. nasolabialis profundus*, a retractor of vibrissae in rows A and B, were observed, as described (Haidarliu et al., 2010).

### Muscles Involved in Aerodynamics Control

In coronal slices that corresponded to the *vestibulum nasi*, an intraturbinate muscle (ITM) was revealed that had not been previously described (Fig. 13). Its fibers originated from the lateral wall of the nostrils, passed medial within the AT, and were inserted into the AT cartilage (Fig. 13B,C).

The appearance of the AT differed from that of the maxillo- and nasoturbinate. The AT was semitransparent, flexible, and separated by an isthmus from the maxilloturbinate (Fig. 2). Bones were not seen in the AT, whereas the rat maxilloturbinate and nasoturbinate contain flat bones (Uraih and Maronpot, 1990; Cho et al., 2000).

In more caudal coronal slices, which contained the *Ductus nasolacrimalis* at the base of the maxilloturbinate, ITM was not detected. At this level, the origins of the Partes anterior et interna of the *M. nasolabialis profundus* were seen attached to the outer wall of the nasal cartilage (Fig. 14). The roof and lateral nasal cartilages were not connected to each other, therefore contraction of the Partes anterior et interna of the *M. nasolabialis profundus* would pull the lateral nasal cartilage outward, which would result in dilation of the nostrils. Simultaneously, the base of the AT could be pulled laterally, which would change the angle and the distance of the AT relative to the septum. As a result, the air streams within the nasal cavity can be modified.

## DISCUSSION

### Involvement of Rostral Snout Muscles in Active Olfactory and Tactile Sensing

The musculature in the DRQ is functionally related to whisking, sniffing, and airflow control, which are important for active touch and olfaction in the rat. Whisking and sniffing are external manifestations of coordinated

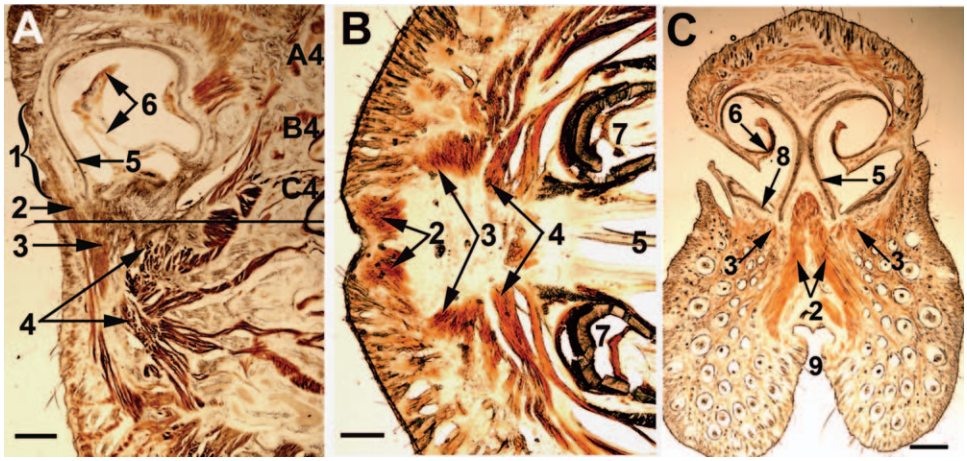


Fig. 8. Appearance of the rostral-most muscles in the rat snout in different planes: oblique (**A**), horizontal (**B**), and coronal (**C**). Slice shown in (B) was obtained by cutting the snout at the level shown by a solid horizontal line in (A). 1, Rhinarium; 2, *M. depressor rhinarii*; 3. *M. depressor septi nasi*; 4, Partes mediae superior et inferior of the *M. nasolabialis profundus*; 5, septal cartilage; 6, atrioturbinate; 7, incisive; 8, medial end of the lateral nasal cartilage; 9, philtrum. A4–C4, vibrissa follicles. Scale bars are 1 mm in (A) and (C), and 0.5 mm in (B).

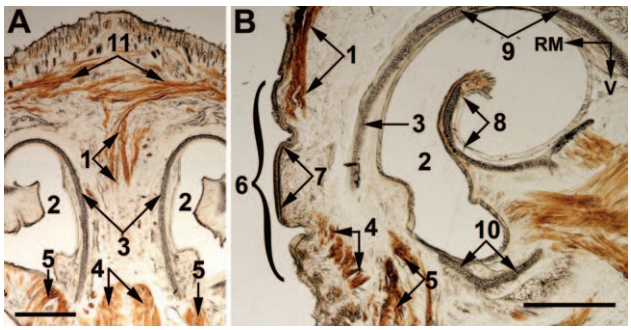


Fig. 9. Coronal (**A**) and oblique (**B**) view of the *M. levator rhinarii* (1) in adult rats. 2, Atrium; 3, rostral splitted part of the septal cartilage; 4, *M. depressor rhinarii*; 5, *M. depressor septi nasi*; 6, rhinarium; 7, tuberculum nasi; 8, atrioturbinate; 9, roof cartilage; 10, lateral nasal cartilage; 11, *M. transverses nasi*. RM, rostromedial; V, ventral. Scale bars = 1 mm.

rhythmic motor activity that involves head, chest, MP, and nose movements (Deschenes et al., 2012). Here, we revealed that the rostral-most muscles that originated from the ventral part of the rhinarium, and from the rostral end of the septum and ventral wall of the vestibulum nasi, were inserted into the upper lip (Fig. 8A,C). In rats, the geometry of these muscles led to the supposition that their contraction may cause ventral deflection of the septum and rhinarium, and a simultaneous uplifting of the upper lip. Rats may also perform dorsal deflection of the nose and rhinarium by contracting *M. dilator nasi* (Fig. 7), and *M. levator rhinarii* (Fig. 9), respectively. All these muscles can participate in fine control of active touch by moving up and down nasal tubercles (Fig. 1), which are supplied with circularly arranged densely innervated epidermal ridges (Macintosh, 1975).

Taking into consideration traditional descriptions of rodent snout musculature, the PIM revealed here may represent a separate slip of the Pars interna of the *M. nasolabialis profundus* (Figs. 11 and 12). Insertion of posterior slips of the *Pars interna* into the MP was reported (Rinker, 1954), but the location of the insertion sites was not. We suppose that the fibers of this slip portion were also divergently directed caudolateral, and were inserted into the capsules of the vibrissae A4 and B4, as well as into the corium in the vicinity of these vibrissae. We referred to this muscle slip as pseudointrinsic, because although it was inserted into the vibrissa capsules, like an IM, it originated from the nasal cartilage, that is, outside the MP, like an extrinsic muscle.

According to Klingener (1964), in *Dipodoids*, a strain of mice that habit grasslands, deserts, and forests, the Pars interna is divided into two parts: a small and deep part that inserts into the tendon of the *M. dilator nas*i, and a larger and superficial part that runs posterodorsally over the *M. dilator nasi* onto the dorsal rostrum. However, according to Rinker (1954), the Pars interna of rodents consists of the following three parts. The most superficial aspect passes caudodorsally onto the bridge of the nose. The least superficial part reaches the bridge of the nose and the tendon of the *M. dilator nasi*. The most posterior aspect enters the MP and also attaches to the lateral border of the same tendon. Our findings confirmed that there are three distinct parts of the Pars interna of the *M. nasolabialis profundus*. Recently, we further described the fourth part, the deepest portion of the Pars interna as a slip that spread caudally and was inserted into the fibrous mat (Haidarliu et al., 2010). The majority of these muscle slips are involved in active tactile and olfactory sensing, and their activity can be modulated by touching (Mitchinson et al., 2011), smelling (Johnson et al., 2003; Wachowiak, 2011), and probably also tasting (Katz et al., 2001; Bahar et al., 2004).

The ITM in rats is described here for the first time (Fig. 13). This muscle arises from the lateral nasal cartilage. Its fibers are directed medial, pass within the AT, and are inserted into the intraturbinate cartilage. ITM-mediated changes in the configuration of the AT could result in the free portion of AT being able to baffle airstreams such that expired gas would be directed laterally, thus less likely to be re-inspired, and inspired air would occur mostly from the rostral (Wilson and Sullivan, 1999).

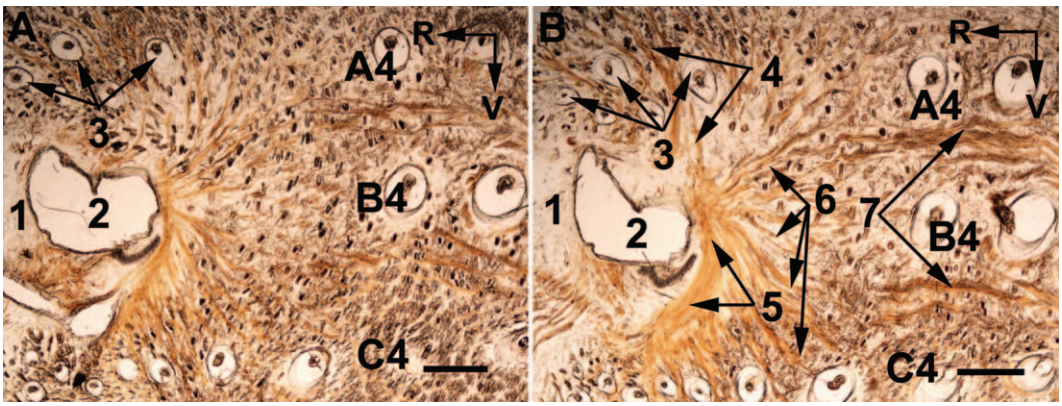


Fig. 10. Light microscopy of tangential slices of the DRQ of an adult rat snout at ~0.3 mm (**A**) and ~0.45 mm (**B**) from the surface of the skin. 1, Rostrum; 2, atrium; 3, nasal vibrissae; 4, Pars interna superficialis, 5, Pars anterior, and 6, posterior slips of the Pars interna of the *M. nasolabialis profundus*; 7, fascicles of the *Mm. nasolabialis et maxillolabialis*. A4–C4, vibrissa follicles; R, rostral; V, ventral. Scale bars = 1 mm.

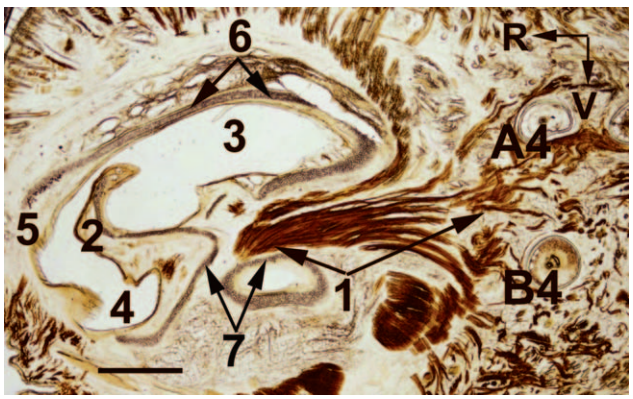


Fig. 11. Light microscopy of a tangential slice of an adult rat snout cut at ~0.6 mm from the surface of the skin. 1, PIM; 2, atrioturbinate; 3, dorsal meatus; 4, ventral meatus; 5, rostrum; 6, roof cartilage; 7, lateral nasal cartilage. A4, B4, vibrissa follicles; R, rostral; V, ventral. Scale bar = 1 mm.

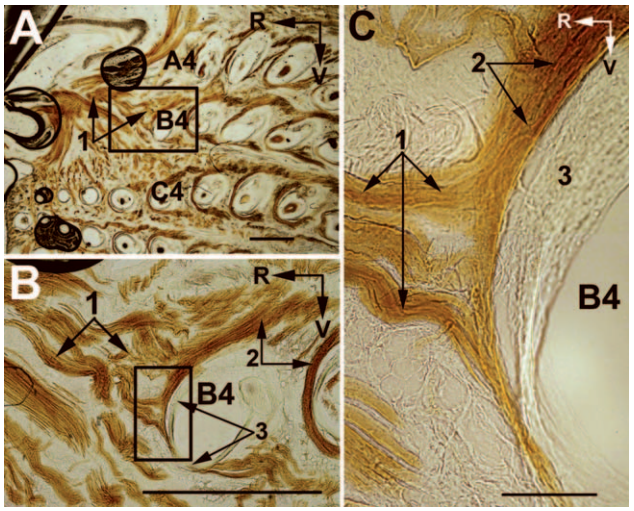


Fig. 12. Light microscopic view of the PIM (1) insertion sites on the capsule (3) of the vibrissa B4 in an adult rat parasagittal slice cut at ~0.8 mm from the surface of the skin. (**A**) An entire slice. (**B**) Higher magnification of boxed area in (A). (**C**) Higher magnification of boxed area in (B). 2, IM. A4–C4, vibrissa follicles; R, rostral; V, ventral. Scale bars are 1 mm in (A) and (B), and 0.1 mm in (C).

During inspiration, the airflow can be baffled such that most of it would be sampled near the rostral part of the snout, be directed into the nostrils, and then through the dorsal medial stream, toward the ethmoidal compartment of the nasal cavity (Fig. 2). We suggest that such a mechanism can occur in parallel to the previously described improvement of odorant detection when the air flow rate over the nostril increases during sniffing (Sobel et al., 2000; Zhao et al., 2005; Oka et al., 2009). During normal respiration, only ~2% of the particle flow in the inspired air reaches the olfactory receptors in humans (de Vries and Stuiver, 1961), and ~1% in dogs (Marshall and Moulton, 1981). In dogs, during sniffing for olfaction, the dorsal meatus acts as a major bypass for odorant-bearing inspired air (Craven et al., 2007).

## Spatial Distribution of Muscle Origins in the DRQ

Most muscles of the DRQ originate from nasal cartilages. Traditionally, the term *M. nasolabialis profundus* designates a large group of muscles in the rostral part of the snout that are spatially separated and fulfill different functions. Based only on dissection, most muscles of the DRQ appear to originate from the lateral nasal cartilage and premaxilla between the incisors (Meinertz, 1944; Rinker, 1954; Klingener, 1964; Ryan, 1989). However, by using serial sectioning, we identified three distinctive and spatially separated areas of the muscle origins in the rostral part of the rat snout that can be seen in a summarizing figure (Fig. 4).

One area was comprising, rhinarium and ventral poles of the septal and lateral nasal cartilages (Figs. 8 and 9; green encircled area in Fig. 4). Originating in this area are two symmetric rostral muscles (*Mm. depressor septi nasi et depressor rhinarii*), and one muscle attached to the dorsal rhinarium (*M. levator rhinarii*).

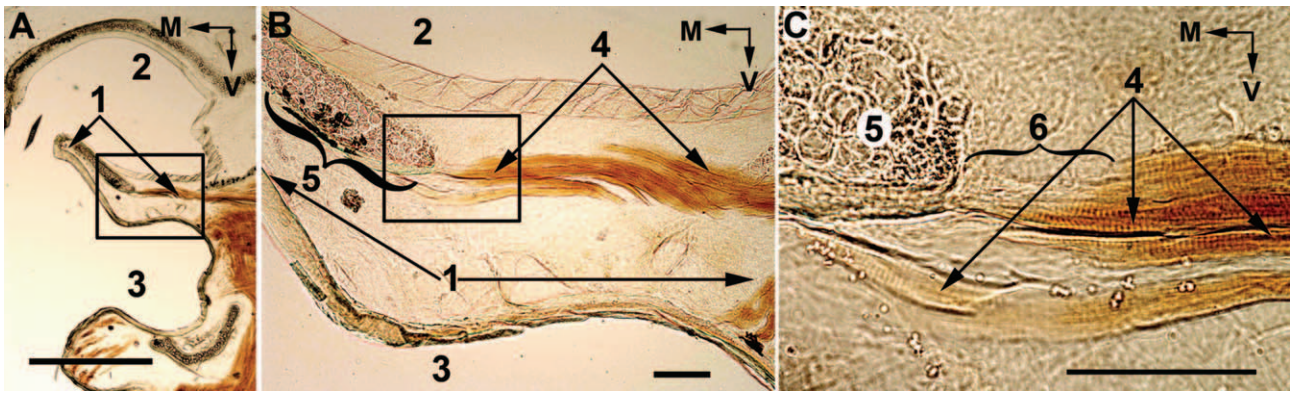


Fig. 13. Light microscopy of a coronal slice prepared from a tissue block containing the lateral wall of the atrium. (**A**) An entire slice; (**B** and **C**) Higher magnifications of the boxed areas in (A) and (B), respectively. 1, Atrioturbinate; 2, dorsal meatus; 3, ventral meatus; 4, ITM; 5, intraturbinate cartilage; 6, site of contact between collagenous structures of the muscle and cartilage. M, medial; V, ventral. Scale bars are 1 mm in (A), and 0.1 mm in (B) and (C).

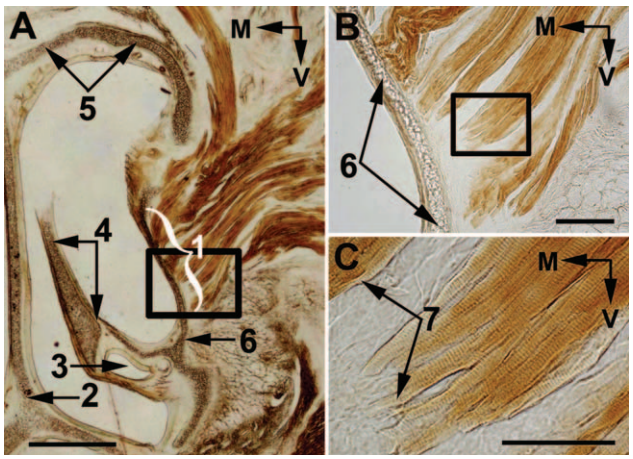


Fig. 14. Light microscopy of an adult rat coronal slice (**A**) that contains origins (1) of the Partes anterior et interna of the *M. nasolabialis profundus*. (**B** and **C**) Higher magnifications of the boxed areas in (A) and (B), respectively. 2, Septal cartilage; 3, ductus nasolacrimalis; 4, maxilloturbinate; 5, roof cartilage; 6, lateral nasal cartilage; 7, sites of muscle attachment to the nasal cartilage. M, medial; V, ventral. Scale bars are 1 mm in (A), 0.2 mm in (B), and 0.1 mm in (C).

These muscles can move the rhinarium up and down, and pull the rostral end of the septum ventrally, enlarging the nostrils, raising the upper lip, and changing the air flow through the nose.

Another area covered the lateral wall of the nasal cartilage, and extended up to the dorsorostral end of the premaxilla (blue encircled area in Fig. 4). The most numerous group of muscles, which are parts of the *M. nasolabialis profundus*, originate in this area. This group of muscle slips includes the Pars anterior, Pars interna, that is, its most superficial, superficial, deep, and caudal (posterior) slips, Partes maxillares superficialis et profunda, as well as the PIM and ITM. In most publications, only the origins and insertion sites of these muscles were mentioned (Meinertz, 1944; Rinker, 1954; Klingener, 1964; Ryan, 1989). A function for this muscle group was not clear. We suggest that the principal function of this muscle group is nostril dilatation, because all these muscles originate on the outer wall of the lateral nasal cartilage, and their insertion sites are located in the corium around the nose. Since the insertion sites of these muscles were located more lateral than their origins, muscle contractions should pull the lateral nasal cartilage outward, so that the nostril becomes dilated. Some of these muscles, that is, a few slips of the Pars interna and PIM, were inserted into MP and could cause simultaneous nasal dilation and vibrissal protraction. Such a dual effect of facial muscle contraction was hypothesized by Wineski (1985). In this group, only three muscles had other functions. The ITM changes the configuration of the AT, and the airflow pattern. The Partes maxillares superficialis et profunda participate in retraction and rostral translation of the vibrissae.

The third area is located on the rostral part of the processus alveolaris of the premaxilla, and involves septum intermusculare (pink encircled area in Fig. 4). From this area arise Partes mediae superior et inferior of the *M. nasolabialis profundus* (Fig. 8A,B). The two latter muscles were represented by seven large flat muscle slips that penetrated between the rows of vibrissae, three directed to the dorsal, and four to the ventral compartment of the MP, and were inserted into the corium of the MP. Contraction of these muscles initiates the first phase of protraction of the vibrissae, and pulls the MP rostral, which causes rostral translation of the vibrissae (Hill et al., 2008).

## CONCLUSIONS

The DRQ of the rat snout is involved in active tactile and olfactory sensing. The DRQ contains muscles that are involved in whisking, sniffing and air flow control. Rostral vibrissae of the MP can be protracted and translated by muscles originating from the nasal cartilage, and inserted into the vibrissa capsules in rows A and B, and into the corium of both the dorsal and ventral compartments of the MP. Lateral and caudal nose movements can be initiated by the *M. dilator nasi* that is inserted into the roof cartilage of the nose. Contraction of the revealed ITM can change the angle of the free portion of the AT relative to the nasal wall and septum, so that the intranasal inspiratory and/or expiratory

airflow patterns can be modified. Two rostral-most muscles can participate in the active rhinarial touch.

## ACKNOWLEDGEMENTS

The authors thank Noam Sobel and Tali Kimchi for valuable discussion, and Barbara Schick for reviewing the manuscript. Ehud Ahissar holds the Helen Diller Family Professorial Chair of Neurobiology.

## LITERATURE CITED

Ahissar E, Knutsen PM. 2008. Object localization with whiskers. Biol Cybern 98:449–458.

Bahar A, Dudai Y, Ahissar E. 2004. Neural signature of taste familiarity in the gustatory cortex of the freely behaving rat. J Neurophysiol 92:3298–3308.

Banke J, Mess A, Zeller U. 2001. Functional morphology of the rostral head region of *Cryptomys hottentotus* (Bathyergidae, Rodentia). In: Proceedings of the 8th International Symposium on African Small Mammals. p 231–241.

Berg RW, Kleinfeld D. 2003. Rhythmic whisking by rat: retraction as well as protraction of the vibrissae is under active muscular control. J Neurophysiol 89:104–117.

Bermejo R, Friedman W, Zeigler HP. 2005. Topography of whisking II: interaction of whisker and pad. Somatosens Mot Res 22: 213–220.

Bojsen-Moller F, Fahrenkrug J. 1971. Nasal swell-bodies and cyclic changes in the air passage of the rat and rabbit nose. J Anat 110: 25–37.

Brácha V, Zhuravin IA, Bureš J. 1990. The reaching reaction in the rat: a part of the digging pattern? Behav Brain Res 36:53–64.

Brecht M, Grinevich V, Jin T-E, Margrie T, Osten P. 2006. Cellular mechanisms of motor control in the vibrissal system. Pflugers Arch: Eur J Physiol 453:269–281.

Breitsprecher L, Fanghänel J, Noe A, Lockett E, Raab U. 2002. The functional anatomy of the muscles of facial expression in humans with and without Cleft Lip and Palate. A contribution to refine muscle reconstruction in primary cheilo- and rhinoplasties in patients with uni- and bilateral complete CLP. Ann Anat 184:27–34.

Carvell GE, Simons DJ. 1990. Biometric analysis of vibrissal tactile discrimination in the rat. J Neurosci 10:2638–2648.

Carvell GE, Simons DJ, Lichtenstein SH, Bryant P. 1991. Electromyographic activity of mystacial pad musculature during whisking behavior in the rat. Somatosens Mot Res 8:159–164.

Cho NY, Hotchkiss JA, Bennett CB, Harkema JR. 2000. Neutrophil-dependent and neutrophil-independent alterations in the nasal epithelium of ozone-exposed rats. Respir Crit Care Med 182:629–236.

Craven BA, Neuberger T, Paterson EG, Webb AG, Josephson EM, Morrison EE, Settles GS. 2007. Reconstruction and morphometric analysis of the nasal airway of the dog (*Canis familiaris*) and implications regarding olfactory airflow. Anat Rec 290:1325–1340.

Deschênes M, Moore JD, Kleinfeld D. 2012. Sniffing and whisking in rodents. Curr Opin Neurobiol 22:243–250.

De Vries H, Stuiver M. 1961. The absolute sensitivity of the human sense of smell. In: Rosenblith WA, editor. Sensory communication. New York: Wiley. p159–167.

Diogo R, Wood BA, Aziz MA, Burrows A. 2009. On the origin, homologies and evolution of primate facial muscles, with a particular focus on hominoids and a suggested unifying nomenclature for the facial muscles of the Mammalis. J Anat 215:300–319.

Dörfl J. 1982. The musculature of the mystacial vibrissae of the white mouse. J Anat 135:147–154.

Grant RA, Mitchinson B, Fox CW, Prescott TJ. 2009. Active touch sensing in the rat: anticipatory and regulatory control of whisker movements during surface exploration. J Neurophysiol 101:862–874.

Haidarliu S, Simony E, Golomb D, Ahissar E. 2010. Muscle architecture in the mystacial pad of the rat. Anat Rec 293:1192–1206.

Haidarliu S, Simony E, Golomb D, Ahissar E. 2011. Collagenous skeleton of the rat mystacial pad. Anat Rec 294:764–773.

Haselton FR, Sperandio PGN. 1988. Convective exchange between the nose and the atmosphere. J Appl Physiol 64: 2575–2581.

Hill DN, Bermejo R, Zeigler HP, Kleinfeld D. 2008. Biomechanics of the vibrissa motor plant in rat: rhythmic whisking consists of triphasic neuromuscular activity. J Neurosci 28: 3438–3455.

Hill DN, Curtis JC, Moore JD, Kleinfeld D. 2011. Primary motor cortex reports efferent control of vibrissa motion on multiple timescales. Neuron 72:344–356.

Huijing PA. 1999. Muscle as a collagen fiber reinforced composite: a review of force transmission in muscle and whole limb. J Biomech 32:329–345.

Johnson BN, Mainland JD, Sobel N. 2003. Rapid olfactory processing implicates subcortical control of an olfactomotor system. J Neurophysiol 90:1084–1094.

Katz DB, Simon SA, Nicolelis MAL. 2001. Dynamic and multimodal responses of gustatory cortical neurons in awake rats. J. Neurosci 21:4478–4489.

Kepecs A, Uchida N, Mainen ZF. 2006. The sniff as a unit of olfactory processing. Chem Senses 31:167–179.

Kepecs A, Uchida N, Mainen ZF. 2007. Rapid and precise control of sniffing during olfactory discrimination in rats. J Neurophysiol 98:205–213.

Klingener D. 1964. The comparative myology of four dipodoid rodents (Genera *Zapus, Napeozapus, Sicista*, and *Jaculus*). Misc Publ Mus Zool Univ Michigan 124:1–100.

Knutsen PM, Ahissar E. 2009. Orthogonal coding of object location. Trends Neurosci 32:101–109.

Knutsen PM, Biess A, Ahissar E. 2008. Vibrissal kinematics in 3D: tight coupling of azimuth, elevation, and torsion across different whisking modes. Neuron 59:35–42.

Komisaruk BR. 1970. Synchrony between limbic system theta activity and rhythmical behavior in rats. J Comp Physiol Psychol 70: 482–492.

Krinke GJ. 2000. The laboratory rat. 1st ed. London: Academic Press.

Macintosh SR. 1975. Observations on the structure and innervations of the rat snout. J Anat 119:537–546.

Maier von W. 2002. Zur functionellen Morphologie der rostralen Nasenknorpel bei Soriciden. Mamm Biol 67:1–17

Marshall DA, Moulton DG. 1981. Olfactory sensitivity to α-ionone in humans and dogs. Chem Senses 6:53–61.

Meinertz T. 1944. Das superfizielle Facialisgebiet der Nager. VII. Die hystricomorphen Nager. Zeitschr Anat Entwicklungsgesch 113:1–38.

Mitchinson B, Grant RA, Arkley K, Rankov V, Perkon I, Prescott TJ. 2011. Active vibrissal sensing in rodents and marsupials. Phil Trans R Soc B 366:3037–3048.

O'Connor DH, Clack NG, Huber D, Komiyama T, Myers EW, Svoboda K. 2010. Vibrissa-based object localization in head-fixed mice. J Neurosci 30:1947–1967.

Oka Y, Takai Y, Touhara K. 2009. Nasal airflow rate affects the sensitivity and pattern of glomerular odorant responses in the mouse olfactory bulb. J Neurosci 29:12070–12078.

Rinker GC. 1954. The comparative myology of the mammalian genera *Sigmodon, Oryzomys, Neotoma*, and *Peromyscus* (Cricetinae), with remarks on their intergeneric relationships. Misc Publ Mus Zool Univ Michigan 83:1–125.

Ryan JM. 1989. Comparative myology and polygenetic systematics of the Heteromyidae (Mammalia, Rodentia). Misc Publ Mus Zool Univ Michigan 176:1–103.

Saban Y, Amodeo CA, Hammou JC, Polselli R. 2008. An anatomical study of the nasal superficial musculoaponeurotic system. Surgical applications in rhinoplasty. Arch Facial Plast Surg 10: 109–115.

Sachdev RNS, Sato T, Ebner FF. 2002. Divergent movement of adjacent whiskers. J Neurophysiol 87:1440–1448.

Silverman RT, Munger BL, Halata Z. 1986. The sensory innervation of the rat rhinarium. Anat Rec 214:210–225.

Simony E, Bagdasarian K, Herfst L, Brecht M, Ahissar E, Golomb D. 2010. Temporal and spatial characteristics of vibrissa responses to motor commands. J Neurosci 30:8935–8952.

Sinis N, Horn F, Genchev B, Skouras E, Merkel D, Angelova SK, Kaidoglou K, Michael J, Pavlov S, Igelmund P, Schaller H-E, Irintchev A, Dunlop SA, Angelov DN. 2009. Electrical stimulation of paralyzed vibrissal muscles reduces endplate reinnervation and does not promote motor recovery after facial nerve repair in rats. Ann Anat 191:356–370.

Sobel N, Khan RM, Hartley CA, Sullivan EV, Gabrieli JDE. 2000. Sniffing longer rather than stronger to maintain olfactory detection threshold. Chem Senses 25:1–8.

Towal RB, Hartmann MJ. 2006. Right-left asymmetries in the whisking behavior of rats anticipate head movements. J Neurosci 26:8838–8846.

Uraih LC, Maronpot RR. 1990. Normal histology of the nasal cavity and application of special techniques. Environ Health Perspect 85:187–208.

Wachowiak M. 2011. All in a sniff: olfaction as a model for active sensing. Neuron 71:962–973.

Waller BM, Vick SJ, Parr LA, Bard KA, Smith Pasqualini MC, Gothard K, Fuglevand AJ. 2006. Intramuscular stimulation of facial muscles in humans and chimpanzees: duchenne revisited and extended. Emotion 6:367–382.

Welker WI. 1964. Analysis of sniffing of the albino rat. Behavior 22: 223–244.

Whidden HP. 2002. Extrinsic snout musculature in Afrotheria and Lipotypha. J Mammal Evol 9:161–184.

Wilson DA, Sullivan RM. 1999. Respiratory airflow pattern at the rat's snout and an hypothesis regarding its role in olfaction. Physiol Behav 60:41–44.

Wineski LE. 1985. Facial morphology and vibrissal movement in the golden hamster. J Morphol 183:199–217.

Zhao K, Dalton P, Yang GC, Scherer PW. 2005. Numerical modeling of turbulent and laminar airflow and odorant transport during sniffing in the human and rat nose. Chem Senses 31:107–118.